AD-A078 889 PRINCETON UNIV NJ DEPT OF MECHANICAL AND AEROSPACE --ETC F/G 21/2
IGNITION AND FLAME PROPAGATION IN SPRAYS.(U)
DEC 79 W A SIRIGNANO , S K AGGARWAL DAAG29-76-G-0266
UNCLASSIFIED MAE-1459 ARO-14052.2-E NL

| OF |
AD
A 078889

END
DATE
FILMED
1-80
DDC

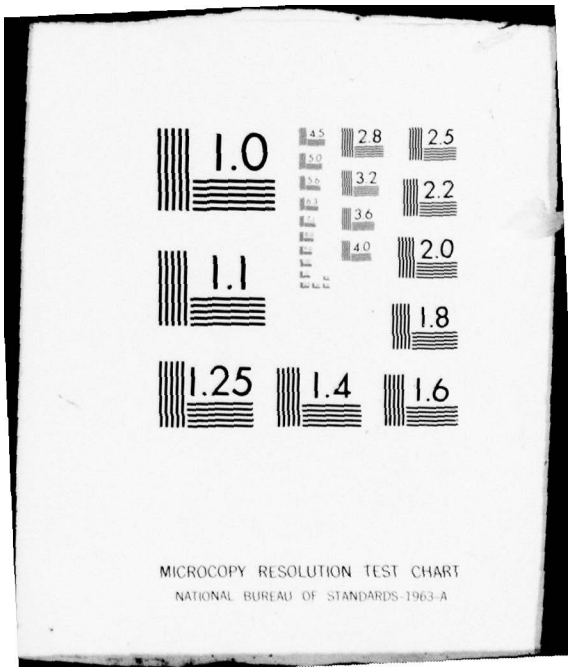
1.0
1.1
1.25
1.4
1.6
1.8
2.0
2.2
2.5
2.8
3.2
3.6
4.0
4.5
5.0
5.6
6.3
7.1
8.0
9.0
MICROCOPY RESOLUTION TEST CHART
NATIONAL BUREAU OF STANDARDS-1963-A

IGNITION AND FLAME PROPAGATION IN SPRAYS

Final Report

Dr. William A. Sirignano
and
Dr. Suresh K. Aggarwal

December 1, 1979

U.S. Army Research Office

Contract/Grant Number
DAAG29-76-G-0266; 77G0145; 78-G-0144

Department of Mechanical and Aerospace Engineering
Princeton University
Princeton, NJ 08544

SECURITY CLASSIFICATION OF THIS PAGE (When Data Entered)

REPORT DOCUMENTATION PAGE

READ INSTRUCTIONS BEFORE COMPLETING FORM

1. REPORT NUMBER: DD1473
2. GOVT ACCESSION NO.
3. RECIPIENT'S CATALOG NUMBER

4. TITLE (and Subtitle): Ignition and Flame Propagation in Sprays.

5. TYPE OF REPORT & PERIOD COVERED: Final Report. 1 June 1976-30 August 1979

6. PERFORMING ORG. REPORT NUMBER: MAE Report No. 1459

7. AUTHOR(s): William A. Sirignano and Suresh K. Aggarwal

8. CONTRACT OR GRANT NUMBER(s): DAAG29-76-G-0266, 77G0145; 78-G-0144 DAAG29-77-G-0145

9. PERFORMING ORGANIZATION NAME AND ADDRESS: Department of Mechanical and Aerospace Eng. Princeton University Princeton, NJ 08544

10. PROGRAM ELEMENT, PROJECT, TASK AREA & WORK UNIT NUMBERS: R&D Project Number 1L161102BH57-06 Mech. and Aero.

11. CONTROLLING OFFICE NAME AND ADDRESS: U. S. Army Research Office Post Office Box 12211 Research Triangle Park, NC 27709

12. REPORT DATE: December 1979

13. NUMBER OF PAGES: 47

14. MONITORING AGENCY NAME & ADDRESS (if different from Controlling Office)

15. SECURITY CLASS. (of this report): Unclassified

15a. DECLASSIFICATION/DOWNGRADING SCHEDULE

16. DISTRIBUTION STATEMENT (of this Report)

Approved for public release; distribution unlimited.

17. 06

18. ARO

19. 14052.2-E

17. DISTRIBUTION STATEMENT (of the abstract entered in Block 20, if different from Report)

NA

14. MAE-1459

18. SUPPLEMENTARY NOTES

The view, opinions, and/or findings contained in this report are those of the author(s) and should not be construed as an official department of the Army position, policy, or decision unless so designated by other documentation.

19. KEY WORDS (Continue on reverse side if necessary and identify by block number)

One-Dimensional Flame Propagation, Ignition, Fyel Sprays, Droplet Vaporization, Combustion, Numerical Modeling, Two Phase Flow

20. ABSTRACT (Continue on reverse side if necessary and identify by block number)

Flame initiation and propagation through an air-fuel vapor-fuel drop system is numerically modeled in a cylindrical one-dimensional combustor. Using an unsteady formulation and allowing unsteady mass, momentum and heat transfer between the two phases, results have been obtained to observe the effects of activation energy, preexponential factor, initial droplet size, initial temperature, stoichiometric ratio and diffusivity on the flame propagation. It is observed that the process is essentially unsteady. Also, unlike pre-mixed →

next page

DD FORM 1 JAN 73 1473 EDITION OF 1 NOV 65 IS OBSOLETE

SECURITY CLASSIFICATION OF THIS PAGE (When Data Entered)

410 732

case, heterogeneous combustion gives rise to large variation in fuel-air ratio, which could produce a secondary diffusion flame in the wake of a propagating flame.

ABSTRACT

Flame initiation and propagation through an air-fuel vapor-fuel drop system is numerically modeled in a cylindrical one-dimensional closed combustor. An unsteady formulation of the flow problem eliminates the cold-boundary difficulty and gas phase ignition problem. A velocity lag between the gas and the liquid phase is allowed and unsteady heat transfer to the droplets is taken into account. The surface temperature of the droplet is evaluated by using an unsteady spherically symmetric formulation of the droplet heat conduction problem with no internal motion and with a time-varying heat flux specified at the surface as a boundary condition. Results have been obtained for two commercially important fuels, namely, n-octane and n-decane. The activation energy and the preexponential factor in the Arrhenius type expression for chemical rate, along with initial temperature, initial droplet size, stoichiometric ratio, and diffusivity are parametrically varied and flame speed and flame temperatures are observed. Flame speed is seen to increase with increasing preexponential factor, with decreasing activation energy, with increasing ambient temperature, with decreasing initial droplet radii, and with increasing diffusivities. It is also observed that unlike premixed combustion, heterogeneous combustion gives rise to local variations in the stoichiometric fuel-to-air ratio in the axial direction. This phenomenon could give rise to a secondary diffusion flame in the wake of a propagating flame and produce local variations in the flame temperature.

TABLE OF CONTENTS

Nomenclature

A	Preexponential constant
B	Spalding transfer number
C_{D_i}	Drag coefficients of i^{th} group of droplets
C_p	Average specific heat at constant pressure
D	Laminar mass diffusivity
F	Heat flux at the droplet surface
F_i	Drag force on i^{th} group of droplets
g	Sum of g_n's, for $n = 1,2,\ldots,\infty$
g_n	Flux integrals arising from unsteady droplet analysis
h	Flux integral arising from unsteady droplet analysis
K	Variable defined as $Tp^{(1-\gamma)/\gamma}$
k	Evaporation constant
k'	Ratio of gas phase to liquid phase thermal conductivity
L	Latent heat of vaporization
ℓ	Length of the combustor
L'_i	Total heat transfer per unit volume to a droplet of group i
$\dot{m}_{v_i}$	Mass vaporization rate from droplet belonging to group i
N	Total number of droplet groups
n_i	Number density of droplets belonging to group i
O	Order of magnitude
P	Pressure
Q	Heat released per unit mass of fuel burnt
R	Gas constant
R_i	Radius of droplets belonging to group i
r	Radial variable in the spherical coordinate system of the droplets
$^{\circ}R$	Universal gas constant

Re_i	Reynolds number of the i^{th} group of droplets
T	Temperature
t	Time variable
T_A	Activation temperature
T_{s_i}	Surface temperature of the i^{th} group of droplets
u	Gas phase velocity
u_{ℓ_i}	Droplet velocity of the i^{th} group of droplets
W	molecular weight
$\dot{W}_{chem_i}$	Mass source of species i per unit volume due to chemical reaction
$\dot{W}_F$	Time rate of change of the fuel mass due to chemical reaction
x	Space variable
Y_i	Mass fraction of species i
$Y_{F_{s_i}}$	Mass fraction of fuel at the droplet surface of the i^{th} droplet group
Z	Functional relating the time derivative of a variable to various variables and their spatial derivatives

Greek Symbols

α	Thermal diffusivity
α_n	n^{th} positive root of the equation $\tan(\alpha) = \alpha$
β	A heat transfer parameter
Γ	Defined as $(1-\gamma)/\gamma$
γ	Specific heat ratio
Δ	Damköhler number
δ	Flame thickness
Δx	Grid spacing in the axial direction
Δt	Grid spacing in the time direction
δ_f	Droplet ignition indicator

δ_{iF}	Kronecker delta
λ	Thermal conductivity
ν	Stoichiometric ratio of fuel mass to oxidizer mass
ρ	Density
τ	Dummy time variable

Subscripts

$\circ$	Initial values
∞	Ambient values
c	Characteristic values
F	Referring to the fuel
i	i^{th} species or i^{th} droplet group
i,j	at i^{th} grid point in x-direction and j^{th} time step
I	Referring to ignition
ℓ	Referring to the liquid phase
N	Referring to the neutral species
O	Referring to the oxidizer
S	Droplet surface

Superscripts

k	Referring to the k^{th} iteration at a fixed time
^	Transformed variables

List of Nondimensionalized Variables

A^*	$= A\rho_c t_c \equiv CB$
D^*	$= Dt_c/L_c^2$
E^*	$= E/(CpT_c)$
F^*	$= Ft_c^2/L_c$
K^*	$= T^*p^{*\Gamma}$
L^*	$= L/(CpT_c)$

$L_i'^* = L_i'/(C_p t_c)$

$n_i^* = n_i L_c^3$

$\dot{m}_{v_i}^* = \dot{m}_{v_i} t_c L_c^3/\rho_c$

$p^* = p/p_c$

$Q^* = Q/(CpT_c)$

$R_i^* = R_i/d_c$

$T^* = T/T_c$

$t^* = t/t_c$

$T_s^* = T_s/T_c$

$T_A^* = E/(^\circ RT_c)$

$u^* = ut_c/L_c$

$u_{\ell i}^* = u_{\ell i} t_c/L_c$

$\dot{W}_F^* = \dot{W}_F t_c/\rho_c$

$x^* = x/L_c$

$\rho^* = \rho/\rho_c$

LIST OF ILLUSTRATIONS

I. INTRODUCTION

Modeling effort in spray combustion has received attention only in the past two or three decades. Although Wolfhard and Parker [1] reported a qualitative study of kerosene spray flame propagation in 1949, the first systematic experimental study was undertaken by Burgoyne and Cohen [2] in 1954. They used small (up to 10 microns diameter) tetralin droplets to study the effect of droplet size on flame speed and concluded that flame speed increases with decreasing droplet size. Similar observations were reported by Mizutani and Ogasawara [3] with much larger droplets (diameter of the order of 100μ). Later Mizutani and co-workers studied the effect of adding relatively nonvolatile fuel droplets to volatile fuel-air mixtures in open burner flames [4], in closed spherical vessels [5], and in spark ignition engines [6]. In each of these situations, the lean flammability limit was extended by such addition, provided the droplet sizes were large enough. For smaller droplets, the behavior shifted towards the premixed behavior. An increase in flame speed was also reported with spray addition. In a similar study, Polymeropoulos and Das [7], by photographic observation of an inverted cone flame using kerosene air spray, concluded that the degree of atomization of spray first increases the flame speed and then decreases it to the premixed combustion value.

By using the principle of the Wilson Cloud Chamber, Hayashi and Kumagai recently obtained a uniformly distributed monodisperse spray of ethanol and n-octane. In their earlier study with this technique [8], using small ethanol droplets, they observed similar effects of droplet size on flame speed as observed in the earlier studies. In their later study [9], with droplets of up to 40 microns diameter, they observed that the presence of liquid phase in lean mixtures resulted in flame speeds smaller than the

premixed flame speed at the same overall fuel mole fraction. The rich mixtures, on the other hand, showed an increase in flame speed compared to the premixed flame speed.

Initial analytic modeling was limited to rather simplified cases due to lack of in-depth understanding of the related processes. Thus, Williams [10] assumed a steady state, monodisperse spray without a velocity lag between the droplets and the gas and analyzed one-dimensional spray deflagration. He further simplified his analysis by assuming the fuel droplets to be either completely vaporized ahead of the flame or negligibly vaporized. In the first case, the flame propagation was essentially premixed, while in the second case a relay mechanism, in which the flame propagated from one droplet to another, was proposed. Inverse proportionality between droplet size and flame speed was obtained for a fixed amount of fuel in the second case. Mizutani [11] performed a much more realistic study by considering a polydisperse spray, turbulent diffusivities, and velocity lag between the gas and the droplets. Droplet temperature was allowed to vary temporally. However, prevaporization was not allowed and a rigorous criterion for droplet ignition was not used; ignition occurred whenever the droplet temperature exceeded a critical value. Flame speed was seen to increase with decrease in droplet size, with increase in turbulent intensity, and with increase in initial temperature. Polymeropoulos [12] analyzed one-dimensional steady-state, laminar flame propagation in a fuel spray system. Prevaporization as well as temporal heating of droplets was allowed. He used the concept of ignition temperature for the droplet ignition and again showed an increase in flame speed with decrease in the droplet diameter up to a droplet size beyond which the flame speed was seen to decrease to the premixed value.

Bracco [13] studied the phenomenon of flame initiation and ignition by treating the gas phase as unsteady. He modeled fuel droplets falling under gravity through a stagnant layer of hot air. The droplets, however, were considered to be at constant temperature and undergoing pure vaporization. The droplet ignition problem was argued to be unimportant. Computations were conducted for cases in which (a) the droplets were completely prevaporized before reaching the hot air zone, (b) were partially prevaporized, and (c) were ignited.

In this report, a numerical study is presented for the combustion of a single-component, polydisperse fuel spray in a one-dimensional closed combustor with laminar flow. The spray is assumed to be dilute so that interaction between the droplets is negligible. Transient heating and pre-vaporization of the droplets is allowed. The coupling between droplet vaporization and environmental conditions, shown to be significant in a cold environment (Law [14]), is considered. Lag between gas and droplet velocities is allowed and the droplet motion is described by a drag law. The effect of convection is described by a Ranz-Marshall type correlation. The need for a gas-phase ignition criterion has been eliminated by an unsteady formulation of the gas phase. The droplet ignition criterion has been based on the concept of ignition Damköhler number, as derived by Law [15]. Using the above model, the phenomena of ignition, flame initiation and propagation have been studied. In addition, the effects of initial temperature, initial droplet size, equivalence ratio, fuel volatility, and activation energy, on these phenomena have been observed.

II. MATHEMATICAL FORMULATION

Firstly, the important assumptions used in the present model will be

listed. Semi-empirical correlations are used in the expressions for droplet drag law and droplet vaporization rate. It is assumed that the viscous dissipation rate is negligible and the kinetic energy of the flow is negligibly small as compared to its thermal energy. As a result, the pressure is assumed to be spatially constant. The wall effects are ignored, i.e., a free slip adiabatic wall is considered. The gas phase is assumed to be thermally and calorically perfect with equal (averaged) specific heats for each species. Binary diffusion coefficients for each pair of species are taken to be equal, thermal diffusion is neglected, and Fick's law of diffusion is employed with the diffusion coefficient taken as a function of temperature and pressure. Also, Fourier's law of heat conduction is used and thermal conductivity is expressed in terms of the diffusion coefficient by assuming the Lewis-Semenov number to be unity. Radiative heat transfer is assumed negligible. Latent heat of vaporization and heat of combustion are assumed constant. The Clasius-Clapeyron relation is used to determine the fuel vapor concentration at the droplet surface. The gas phase chemical reaction is assumed to be governed by a single-step second-order kinetics of the type;

$$\text{Fuel} + \text{Oxidizer} \rightarrow \text{Products}$$

Further, in the analysis of the liquid phase, the gas film surrounding the droplet is considered as quasi-steady. The polydisperse spray has been approximated by superposition of mono-disperse sprays.

Two basic approaches have been used in the literature to formulate the spray combustion problem. The first approach is to consider a steady-state flow problem and thus solve a set of ordinary differential equations. The formulation is faced with the cold boundary difficulty, which is usually removed by suppressing the chemical reactions and droplet vaporization below

certain temperature. The second approach, adopted in the present formulation, treats the whole gas phase problem as unsteady. This approach has wider application and is easier to handle numerically.

Gas-Phase Flow Equations

Considering the source terms due to evaporation and heat transfer from the droplets, and using the assumptions listed above, we can obtain the following conservation equations (Reference 16) for the overall mass density (ρ), species mass fractions (Y_i), momentum and energy respectively:

$$\frac{\partial \rho}{\partial t} + \frac{\partial}{\partial x}(\rho u) = n\dot{m}_v = \sum_{i=1}^{N} n_i \dot{m}_{v_i} \tag{1}$$

$$\frac{\partial(\rho Y_i)}{\partial} + \frac{\partial}{\partial x}(\rho u Y_i) - \frac{\partial}{\partial x}\left(\rho D \frac{\partial Y_i}{\partial x}\right) = \delta_{iF} n\dot{m}_v + \dot{W}_{chem_i} \tag{2}$$

where i corresponds to fuel, oxidizer and product respectively.

$$\frac{\partial p}{\partial x} = 0 \tag{3}$$

$$\rho C_p \frac{\partial T}{\partial t} + \rho C_p u \frac{\partial T}{\partial x} - \frac{\partial}{\partial x}\left(\rho D C_p \frac{\partial T}{\partial x}\right) - \frac{dp}{dt} = \dot{W}_F Q - \sum_{i=1}^{N} n_i \dot{m}_{v_i} [C_p(T-T_{s_i}) + L_i'] \tag{4}$$

Also we have the ideal gas equation

$$p = \rho \frac{^\circ R}{W} T \tag{5}$$

δ_{iF} in Equation (2) is the kronecker delta and is 1 when i equals F and is 0 otherwise. L_i' in Equation (4) is the effective latent heat of vaporization and includes unsteady conduction of heat to the droplets. The source terms in Equations (1) to (4) are given as

$$\dot{m}_{v_i} = (1 + .3\sqrt{Re_i})4\pi R_i \rho D \ \ell n\left(\frac{1-Y_F(1-\delta_f)+\nu\delta_f Y_o}{1-Y_{Fs_i}}\right) \tag{6}$$

$$L_i' = \frac{(1-Y_{Fs_i})\{C_p(T-T_{s_i})+\nu\delta_f Y_o Q\}}{Y_{Fs_i} + \nu\delta_f Y_o - Y_F(1-\delta_f)} \tag{7}$$

$$\dot{W}_F = \frac{A}{W_o}\rho^2 Y_o Y_F e^{-E/^\circ RT} \tag{8}$$

Both $\dot{m}_{v_i}$ and L_i' are obtained (Reference 17) through a quasi-steady analysis of gas phase surrounding a droplet. $\delta_f = 0$ corresponds to the pure vaporization case, whereas $\delta_f = 1$ corresponds to the droplet burning case. The value of δ_f is determined by a droplet ignition criterion, as obtained by Law [15]. Y_{Fs_i}, the fuel vapor mass fraction at the droplet surface is related to T_{s_i} through the Clasius-Clapeyron relation.

An additional equation for pressure is obtained by integrating the energy equation. Using the facts that pressure is a function of time only, velocities vanish at the closed ends of the combustor and that there is no heat loss from the ends of the combustor, Equation (4) can be integrated to yield

$$\frac{dp}{dt} = \frac{\gamma-1}{\ell}\left\{Q\int_o^\ell \dot{W}_F dx - \int_o^\ell \sum_{i=1}^{N} n_i \dot{m}_{v_i}(L_i' - T_{s_i})dx\right\} \tag{9}$$

Similarly, integration of the overall continuity equation yields the expression for the gas velocity

$$u(x) = \frac{1}{\rho(x)}\left\{\int_o^x n\dot{m}_v dx - \frac{\partial}{\partial t}\int_o^x \rho dx\right\} \tag{10}$$

It was anticipated by studying the nature of the first integral on the right hand side of Equation (9) and later verified by computer results that considerable error could be caused in the numerical evaluation of this term [18].

A better approach is to use Equation (10) at $x = \ell$, i.e.,

$$u(\ell) = \frac{1}{\rho(\ell)} \left\{ \int_0^{\ell} n\dot{m}_v dx = \frac{\partial}{\partial t} \int_0^{\ell} \rho dx \right\} = 0 \tag{11}$$

The above equation has been equated to zero since the velocity is identically equal to zero at the closed end ($x = \ell$). The gas density ρ is determined if the gas temperature, the pressure and the gas composition is known through the perfect gas equation. The temperature and the composition are known from the solutions of the energy and species continuity equations, respectively. Equation (11) can thus be used to evaluate pressure. It may be noted that for a combustor open at $x = \ell$, the pressure becomes a constant and then $u(\ell)$ can be obtained by using Equation (10).

Using the transformation:

$$K \equiv Tp \frac{1-v}{v} = Tp^{\Gamma} \tag{12}$$

the energy equation (4) is rewritten as

$$\frac{\partial K}{\partial t} + u \frac{\partial K}{\partial x} - K \frac{\partial}{\partial x} \left(\frac{D}{K} \frac{\partial K}{\partial x} \right) = p^{\Gamma} \frac{\dot{W}_F Q}{\rho} - \sum_{i=1}^{N} \frac{n_i \dot{m}_{v_i}}{\rho} \{ K - p^{\Gamma} (L_i' - T_{s_i}) \} \tag{13}$$

This eliminates the pressure term in the energy equation.

Liquid-Phase Equations

For each group of monodisperse droplets, the general spray distribution function, which may be a function of time, distance, velocity, and radii of the droplets, can be separated into three simpler equations. These three equations, expressing the conservation of droplet number density, droplet mass and droplet momentum, are as follows:

$$\frac{\partial n_i}{\partial t} + \frac{\partial (n_i u_{\ell i})}{\partial x} = 0, \quad i = 1,2,\ldots,N \tag{14}$$

$$\frac{\partial R_i}{\partial t} + u_{\ell_i} \frac{\partial R_i}{\partial x} = - \frac{\dot{m}_{v_i}}{4\pi R_i^2 \rho_{\ell}}, \quad i = 1,2,\ldots,N \tag{15}$$

$$\frac{\partial u_{\ell i}}{\partial t} + u_{\ell i} \frac{\partial u_{\ell i}}{\partial x} = Fi, \qquad i = 1,2,\ldots,N \tag{16}$$

where

$$Fi = \frac{81}{8} \frac{\rho}{(Re_i)\cdot 8 \rho_\ell R_i^2} (u-u_{\ell i})|u-u_{\ell i}| \tag{17}$$

Re_i is the Reynolds number based on the gas kinematic viscosity, the droplet relative velocity and the droplet size.

Assuming that T_{s_i} is known (discussed in the following subsection), we then have (3N+8) variables, i.e., 3N spray variables, n_i, R_i and U_i, three species mass fractions Y_F, Y_O and Y_N, gas velocity u, gas temperature T, gas pressure p, gas density ρ, and thermodynamic variable K. Equations (2), (5), (10) through (16) give a system of (3N+8) equations for these unknowns. The initial profiles of all variables are taken to be uniform in the combustor. Further, the initial gas and droplet velocities are assumed to be zero. The boundary conditions are provided as follows:

<u>At x = 0</u>

$$\frac{\partial Y_F}{\partial x} = \frac{\partial Y_O}{\partial x} = \frac{\partial Y_N}{\partial x} = \frac{\partial K}{\partial x} = u = u_{\ell i} = 0$$

$$n_i = n_{io}$$

$$R_i = R_{io} - \int_o^t \frac{\dot{m}_{v_i}}{4\pi R_u^2 \rho_\ell} dt \tag{18}$$

<u>At x = ℓ</u>

$$\frac{\partial Y_F}{\partial x} = \frac{\partial Y_O}{\partial x} = \frac{\partial Y_N}{\partial x} = \frac{\partial K}{\partial x} = 0$$

<u>Droplet Surface Temperature</u>

Accurate determination of the droplet surface temperature under vaporizing and combusting conditions is very important in spray combustion modeling.

In many practical applications, droplets undergo a period of pure vaporization before ignition takes place. The instant at which a flame is established around the droplets depends on many ambient properties, including temperature and fuel concentration. The amount of vapor fuel depends on the rate at which a droplet vaporizes, which in turn, is a strong function of droplet surface temperature. Since many of the droplet characteristics change significantly upon ignition, it is obvious that the surface temperature histories have to be evaluated accurately. This makes the treatment of the droplet heat transfer problem necessarily unsteady.

Further, in considering a realistic multicomponent fuel droplet, where vaporization rates of different components depend on their distribution within the droplet, determination of the temperature profiles in the interior of the droplet is essential [19,20,21]. Although in the present study we are considering only monocomponent fuel droplets, the extension of the present model to the case of multicomponent fuel droplets is of interest. We will analyze droplet transient heating in the limit of pure conduction where variation in temperature is possible in the interior of the droplet. Results for the more realistic case of axisymmetric internal circulation inside the droplet have been obtained recently (Prakash and Sirignano [22,23]). However, these results were not available at the time this model was formulated and we have employed the results of Law and Sirignano [24] and Law [25]. The details of the droplet energy equation with appropriate boundary conditions are given in Reference [18]. The solution of that equation with a constant heat flux at the surface can be found in Carslaw and Jaeger [26]. For time varying surface heat flux $\hat{F}(t)$ an analytical solution is obtained by using Duhamel's Principle.

Thus, for the surface temperature of the droplet, the following expression is obtained.

$$\hat{T}(\hat{r},\hat{t}) = [\frac{5\hat{r}^2-3}{10} - \frac{2}{\hat{r}} \sum_{n=1}^{\infty} \frac{\sin \hat{r}\alpha_n}{\alpha_n^2 \sin \alpha_n}]\hat{F}(\hat{t}) + 3\int_o^t \hat{F}(\tau)d\tau$$

$$+ \frac{2}{\hat{r}} \sum_{n=1}^{\infty} \frac{\sin \hat{r}\alpha_n}{\sin \alpha_n} \int_o^{\hat{t}} \hat{F}(\tau)e^{-\alpha_n^2(t-\tau)} d\tau \qquad (19)$$

where α_n, $n = 1,2,\ldots,\infty$ are positive roots of the equation

$$\tan \alpha = \alpha. \qquad (20)$$

For a large enough number N_o, for which $\alpha_{N_o}^2 >> 1$, the above equation can be written with finite sum as

$$\hat{T}_s(\hat{t}) = C_1\hat{F}(\hat{t}) + 3\int_o^{\hat{t}} \hat{F}(\tau)d\tau + 2 \sum_{n=1}^{N_o} \int_o^{\hat{t}} \hat{F}(\hat{t})e^{\alpha_n^2(\hat{t}-\tau)} d\tau \qquad (21)$$

where

$$C_1 = 0.2 - 2 \sum_{n=1}^{N_o} 1/\alpha_n^2 \qquad (22)$$

The integrals present in Equation (21) cannot be directly evaluated numerically in convective situations, since the equation has been derived in coordinates fixed to a droplet whereas the flow equations are obtained in the coordinates of the combustor in which the droplets are moving. In a numerical scheme, the integrands can be calculated only at discrete grid points and cannot follow a droplet unless an extensive interpolation scheme is used to approximate the values between the grid points. A more accurate approach is to calculate the integrals by solving the differential equations obtained from a transformation which relates the two coordinate systems. We define new variables $\hat{h}(\hat{t})$ and $\hat{g}(\hat{t})$ as

$$\hat{h}(\hat{t}) = \int_o^{\hat{t}} \hat{F}(\tau)d\tau \qquad (23)$$

and

$$\hat{g}(\hat{t}) \equiv \sum_{n=1}^{N_o} \hat{g}_n(t) \equiv \sum_{n=1}^{N_o} \int_o^{\hat{t}} \hat{F}(\tau) e^{-\alpha_n^2 (t-\tau)} d\tau \tag{24}$$

Under the transformation from the frame of reference of the moving droplet to the frame of reference of the combustor, the variables $\hat{T}_s(\hat{t})$, $\hat{F}(\hat{t})$, $\hat{h}(\hat{t})$ and $\hat{g}(\hat{t})$ transform into $T_s(t,x)$, $F(T,x)$, $h(t,x)$ and $g(t,x)$, respectively. The following differential equations for h and g can be immediately written

$$\frac{\partial h}{\partial t} + u_\ell \frac{\partial h}{\partial x} = \frac{\alpha_\ell}{R^2} F(t,x) \tag{25}$$

$$\frac{\partial g_n}{\partial t} + u_\ell \frac{\partial g_n}{\partial x} + \frac{\alpha_\ell}{R^2} \alpha_n^2 g_n = \frac{\alpha_\ell}{R^2} F, \qquad n = 1,2,\ldots,N_o \tag{26}$$

Thus the integrals in Equations (21) can be evaluated by solving equations (25) and (26). The boundary conditions for these equations are easily obtained, realizing that $u_\ell = 0$ at the $x = 0$ boundary, by direct integration of Equations (25) and (26) which gives $h(0,t)$ and $g_n(0,t)$, $n = 1,2,\ldots,N_o$. T_s is then given by

$$\hat{T}_s(\hat{t}) = (0.2 - 2 \sum_{n=1}^{N_o} 1/\alpha_n^2)\hat{F} + 3\hat{h} + 2\hat{g} \tag{27}$$

III. NUMERICAL CONSIDERATIONS

The final set of governing equations are first nondimensionalized with respect to appropriate characteristic values so that all variables are of the same order of magnitude. The characteristic values are based on the phenomenon of interest. Thus, the characteristic value of distance is based on the flame thickness and the characteristic value of time is based on the values of diffusion, vaporization, and chemical times. Using the variables in the ignition zone, these are estimated to be

$$\delta \sim \sqrt{D\dot{W}_F} \qquad \sim O(0.2 \text{ cm.})$$

$$\tau_{diffusion} \sim \frac{\delta^2}{D} \qquad \sim O(0.1 \text{ sec.})$$

$$\tau_{vaporization} \sim \frac{4r_o^2}{k} \qquad \sim O(0.01 \text{ sec.})$$

$$\tau_{chemical} \sim \frac{\rho Y_F}{\dot{W}_F} \qquad \sim O(0.001 \text{ sec.})$$

The characteristic values of other variables such as pressure, temperature, density, droplet size, etc., are conveniently chosen at their initial ambient values and the characteristic values of derived quantities are obtained from dimensional considerations.

Since the governing equations constitute a set of nonlinear partial differential equations, it would be easier to solve them if they are linearized in some way. We will be using the technique of quasi-linearization, first introduced by Bellman and Kalaba [27] and later used by Lee [28] and Sharma and Sirignano [29].

In this technique, the nonlinear terms are expanded in a Taylor series with respect to the variable and its derivatives around the previously known value. Thus, for a typical non-linear differential equation

$$\frac{\partial Y}{\partial t} = Z(Y, Y_x, Y_{xx}) \tag{28}$$

the quasi-linearized form is

$$\left(\frac{\partial Y}{\partial t}\right)^{k+1} = Z^k + \left(\frac{\partial Z}{\partial Y}\right)^k (Y^{k+1} - Y^k) + \left(\frac{\partial Z}{\partial Y_x}\right)^k (Y_x^{k+1} - Y_x^k) + \left(\frac{\partial Z}{\partial Y_{xx}}\right)^k (Y_{xx}^{k+1} - Y_{xx}^k) \tag{29}$$

where subscript x represents the partial derivative with respect to x, superscript k refers to a previously known value and (k+1) refers to an

unknown value. This linearization process has an added advantage of generating a set of uncoupled differential equations. These equations, when approximated by an implicit finite difference method, leads to a tridiagonal matrix as opposed to the linearization technique, used by Briley and McDonald [30], which leads to a block tridiagonal system. However, the present method needs iteration to obtain the solution at each time step.

The quasi-linearized equations were replaced by finite-difference approximations by employing an implicit scheme, similar to Crank-Nicolson scheme. However, it was observed that the scheme, when used for the first spatial derivative, lead to an oscillatory behavior for the variables governed by first order differential equations. A satisfactory analog for the first derivative was found to be as follows:

$$\left(\frac{\partial Y}{\partial x}\right)_{i,j+1/2} = \frac{Y_{i,j+1} - Y_{i-1,j+1} + Y_{i+1,j} - Y_{i,j}}{2\Delta x} + O(\Delta t \cdot \Delta x) \tag{30}$$

where the subscripts i and j represent, respectively, the $i\Delta x$ and $j\Delta t$ locations in space and time. Then the finite-difference approximation to Equation (29) is

$$C^k Y^{k+1}_{i-1,j+1} + A^k Y^{k+1}_{i,j+1} + B^k Y^{k+1}_{i+1,j+1} = D^k \tag{31}$$

where Y^{k+1} is the unknown variable which is being solved at each of the grid points and A^k, B^k, C^k and D^k are coefficients calculated from the known values of the variables at the previous iteration. If ID is the total number of grid points then we can obtain ID-2 such equations for $i = 2,3,\ldots,ID-1$. Boundary conditions provide two more equations. Thus we have ID equations for ID unknowns Y^{k+1}.

Flame initiation has been modeled by providing a zone of heated gases at one end of the combustor. A temperature of 1500°k and a length of

one half cm for the hot zone has been found sufficient for ignition in most cases. A corresponding amount of fuel has been removed from the hot zone so as to maintain the adiabatic flame temperature the same. To avoid large gradients near the ignition source, the initial values of all variables are varied linearly from the ignition source values to ambient values in the next one-half centimeter. Then using Equation (31) with boundary conditions (18), the variables Y_F, Y_O, Y_N, k, n_i, R_i and u_{ℓ_i} are sequentially solved. New pressure and velocity values are obtained from Equations (11) and (10), and T_{s_i} is obtained from Equations (25), (26) and (27). Again, an implicit numerical scheme is used to solve Equations (25) and (26). Once all variables are known at $k+1^{st}$ iteration, new coefficients for Equation (31) are obtained. This process is repeated until convergence is achieved at each of the grid points for a given time. Then time is incremented and the same process is repeated. To check the accuracy of the method, the value of Y_N, as obtained by solving equation for Y_N, is compared with the value of the same as obtained from relation $Y_N = 1 - Y_F - Y_O$.

The grid spacings in the space and time axes, i.e., Δx and Δt, have been based on the characteristic values of length and time. The value of Δt varies from one-half millisecond to 10 microseconds depending on the characteristic value of the chemical and evaporation times for various cases. Another consideration for choosing Δt is the cost. A smaller Δt requires fewer quasilinearization iterations (k-iterations) at any time and vice versa. Although a rigorous criterion for determining Δt has not been derived, experience shows that modeling is most economical when the number of k-iterations at any time lies between 2 to 5. It may be noted here that in some of the cases when time steps of the order of 10 microseconds must be

chosen, complete flame propagation in the combustor may require as many as 10,000 time iterations (approximately $3 * 10^4$ k-iteration). Therefore, in many cases modeling has been terminated when the flame has propagated a significant portion of the combustor length.

The values of physio-chemical constants for the fuel and the ambient gas have been compiled from various sources [30,31,32]. Some variation was seen in the values of the latent heat of vaporization and heat of combustion of the fuel. Therefore, whenever possible, all data for a fuel has been collected from a single source. The averaged constant value of C_p is selected to yield the adiabatic flame temperature upon complete combustion of stoichiometric fuel mixture. In reality, value of C_p depends on the gas temperature and, to a lesser degree, on the gas pressure and composition. Therefore a constant C_p would not yield accurate results for incomplete combustion, different stoichiometric ratios or different initial conditions.

Cases with various values of the preexponential factor A, activation energy E, initial temperature, T_0, overall equivalence ratio ϕ, diffusivity D, droplet size R, and cases of homogeneous combustion have been modeled. Parametric variation of A and E is important since the value of these parameters, for the fuels under consideration, is not known with much confidence.

IV. RESULTS AND DISCUSSION

Before we discuss the results, it may be indicated that after all the above mentioned cases had been calculated, some errors were found in the computer code. In addition, few modifications were incorporated in the code.

For example, the finite difference scheme for the liquid phase equations and the droplet surface temperature equations was made second order accurate. This resulted in a reduction of observed flame speed as the amount of numerical diffusion was reduced. Other modifications were aimed at making the code more efficient. It is expected, though not claimed, that all these alterations will effect only the quantative nature of the results obtained from the old code. Consequently, only one control case for n-Decane fuel droplets of 40μ radius has been repeated with the new code. All the other results and conclusions have been derived from the old code. The results of the repeated case are shown in Figures 1a to 1h, where the profiles of fuel main functions, oxidizer mass friction, gas temperature, gas velocity, droplet velocity, droplet number density, droplet radius and the reaction rate are plotted in the combustor for several time values. The grid size for this control run was .625 mm and the time step varied from 10μs to 100μs. It was observed, through trial and error, that the characteristic reaction time controlled the time step.

Figures 1a, 1b and 1c indicate some distinguishing features of flame propagation in air-fuel spray mixtures. Firstly, as seen in Figure 1a and 1b, the mixture equivalence ratio, which, initially is less than unity everywhere in the combustor, can greatly vary along the length of the combustor at later times. Secondly, the present results indicate the presence of a secondary diffusion flame in the wake of the primary propagating flame. The location of the primary flame, a pre-mixed type flame, is indicated by a sharp peak in the fuel mass fraction profiles. This sharp peak is caused by the suddenly enhanced vaporization rate in the vicinity of the primary flame. The location of the secondary flame, a diffusion type flame, is the point

where both the fuel and oxidizer mass fractions vanish. This location is particularly evident in the profiles for $t \geq 104$ ms in Figures 1a and 1b. Also, the first peak in the temperature profiles for $t \geq 104$ ms indicates this diffusion flame. The above features can be attributed to the relative motion of the gas and the droplets. This relative motion is demonstrated in Figures 1d and 1e. In these figures, the point where the velocity reverses sign represents the location of the primary flame. Thus, the flows of gas and droplets are always away from the primary flame. However, in case of the secondary diffusion flame, fuel and oxidizer flow towards the flame.

In the colder or upstream section of the combustor, gas temperature rises, as indicated by Figure 1c, due to adiabatic compression of the gas. This enhances the heat transfer rate to the droplet. As a consequence, the droplet surface temperature rises, which, in turn, increases the droplet vaporization rate in the colder region. In addition, because the droplets move away from the flame, the droplet number density increases, in the colder region of the combustor (see Figure 1f). This further enhances the vaporization rate in that region. Consequently, as seen in Figure 1g, the droplet radius decreases at a continuously increasing rate in that region.

It is also worth mentioning that Figure 1f exhibits an oscillatory behavior for the droplet number density near the combustor ends. This is acceptable near the left end as the droplet radius, there, is negligibly small. The oscillatory behavior near the right end is possibly due to some inconsistency in using the boundary conditions for the liquid phase equations. This is, presently, under investigation. Profiles of the surface temperature of the droplets were qualitatively similar to the gas

temperature profiles. The maximum value of droplet temperature, however, was limited by the boiling point of the fuel.

The reaction rate profiles, shown in Figure 1h, indicate a very narrow reaction zone for the primary flame. Consequently, the time step and the grid size for the finite difference equations were controlled by the thickness of this reaction zone. The presence of the secondary flame, a diffusion type flame moving in a direction opposite to that of the primary flame, is also indicated, in Figure 1h, by the non-zero reaction rates near $x = 2$ cm and for $t = 160$ and 580 ms. The reaction rate profiles for the primary flame also demonstrate the unsteady nature of flame propagation in sprays. The maximum value of the reaction rate shows a wide variation as the primary flame propagates through the combustor. This variation is related to the variation in the local equivalence ratio of the mixture (ϕ) in the vicinity of the primary flame. Table I lists these ϕ values along with the values of the maximum reaction rate. As this table indicates, the value of the maximum reaction rate rises as ϕ approaches unity. This variation in the reaction rate is also responsible for the peculiar nature of the temperature profiles between the two temperature peaks corresponding to the primary and secondary flames (see Figure 1c). For example, for the profile at $t = 580$ ms, the low temperature point between the two peaks is due to the fact that the maximum value of reaction rate at earlier times, say at $t = 160$ and 320 ms, was relatively small. The unsteady nature of the flame propagation is also manifested in Table II, which gives the flame location, the flame velocity relative to the combustor, the gas velocity and the flame front velocity relative to the gas for several t values. All these values pertain to the primary flame. The flame location is defined as the point where the gas temperature is 1000°k. The variation

in the flame velocity relation to gas is related, through the reaction rate, to the variation in the local equivalence ratio.

In the rest of this section, the effects of varying A, E, T_o and D are discussed. The results of two other runs, one with a pre-mixed homogeneous mixture and the other with two mono-disperse droplet groups, are also mentioned. Since all of these results were obtained by using the older version of the computer code, only a qualitative discussion can be given with confidence.

A reduction in preexponential factor A caused a reduction in the observed flame velocities. This could lead to an extinguishment of the flame. A reduction in activation energy E had just the opposite effect. In addition, the secondary diffusion flame would appear earlier if E is reduced. The effect of increasing the initial gas temperature T_o, from 300°k to 600°, is shown, again qualitatively, in Figures 2a and 2b. These figures indicate that the variation in the equivalence ratio is not quite as severe as in the control run. The reason is the enhanced heat transfer rate to the droplets, which increases the vaporization rate in the colder part of the combustor. In other words, there is a tendency to approach the case of pre-mixed homogeneous type of combustion away from the ignition source. For moderate increase in T, however, we still have a fuel rich region near the ignition source and an oxidizer-rich region, formed behind the primary flame as this flame travels into the fuel-lean region. A diffusion type flame appears at the interface of these two regions. The effects of increasing mass and thermal diffusion coefficients were, as expected, an increased flame speed and an increased flame thickness.

Figure 3 gives the temperature profiles for the flame propagation in a pre-mixed homogeneous mixture. Again the results are only qualitatively correct. Important features are: (1) As expected, there is no secondary

diffusion flame and (2) the primary flame tends to propagate with a relatively steady velocity.

A case of two mono-disperse droplet groups, which represents the simplest poly-disperse case, was also modeled. Initial droplet sizes of 40μ and 20μ were used. A reduction in droplet size resulted in an increase in flame speed. Droplet radius and velocity profiles are shown in Figures 4a and 4b, respectively. Figure 4b indicates that the smaller droplets can follow the gas more easily.

CONCLUSIONS

The phenomenon of one-dimensional flame propagation in air and fuel spray mixtures, with transient heating of the droplets allowed, have been successfully modeled. Some preliminary results have been reported. These results are more useful for studying the processes involved in a qualitative way rather than for making quantitative predictions. It is clear that the process is essentially unsteady for all the cases considered with the exception of pre-mixed case. The unsteadiness is due to (a) the time-varying stratification caused by the motion of the droplets and (b) the transient heating of the droplets.

Before obtaining more detailed and quantitatively useful results, further refinement and optimization of the computer code is worth considering. For example, a non-iterative, fully-implicit scheme, as use by Briley and McDonald [30], as well as a variable grid size may be worth investigation. In future work, one could:

I. Relax the non-essential assumptions like constant C_p.

II. Include the effect of turbulence, say, by using a k-ε type model.

III. Consider certain realistic effects such as (a) addition of gravity, (b) addition of wall heat transfer, (c) spark ignition process and (d) a combustor open at both ends, useful for studying the properties of steady flames. For case III(d), the effect of droplet diameter, droplet number density, overall equivalence ratio and fuel volatility on mechanism of flame propagation, flame speed and flammability limits can be studied.

ACKNOWLEDGMENT

This study has been supported by the Army Research Office under Grant DAAG29-78-G-0144.

Table I

t = 10 ms $\dot{W}_{max}$ = .031		t = 30 ms $\dot{W}_{max}$ = .08		t = 160 ms $\dot{W}_{max}$ = .004		t = 320 ms $\dot{W}_{max}$ = .004		t = 460 ms $\dot{W}_{max}$ = .02		t = 580 ms $\dot{W}_{max}$ = .053		t = 680 ms $\dot{W}_{max}$ = .05	
T	ϕ	T	ϕ	T	ϕ	T	ϕ	T	ϕ	T	ϕ	T	ϕ
1197	3.9	1322	3.7	1087	.40	1014	.40	1200	.5	1863	.5	1875	.3
837	1.8	950	1.2	870	.45	859	.46	880	.7	980	.93	985	.85
622	.90	671	.95	642	.48	726	.50	687	.72	605	.93	579	.9
480	.50	501	.75	519	.5	615	.55	540	.77	448	.85	441	.87
380	.25	398	.40	435	.49	525	.58	410	.75	390	.8	396	.81

$\dot{W}_{max}$ = Maximum value of the Non-Dimensional Reaction Rate

Table II. Flame Velocity for the Control Run

TIME (t in ms)	x_{1000} = Location of T = 1000°k (cm)	Flame Velocity cm/sec Relative to Combustor	Gas Velocity cm/sec	Flame Velocity cm/sec Relative to Gas
0	.62			
6	.844	37.0	9.3	27.7
20	1.28	31.3	7.7	23.6
110	2.94	18.4	1.6	16.8
160	3.25	6.2	.5	5.7
300	3.75	3.6	.4	3.2
460	4.53	5.0	2.4	2.6
580	5.87	11.2	2.4	8.8
680	6.25	8.8	2.0	6.8

Figure 1a

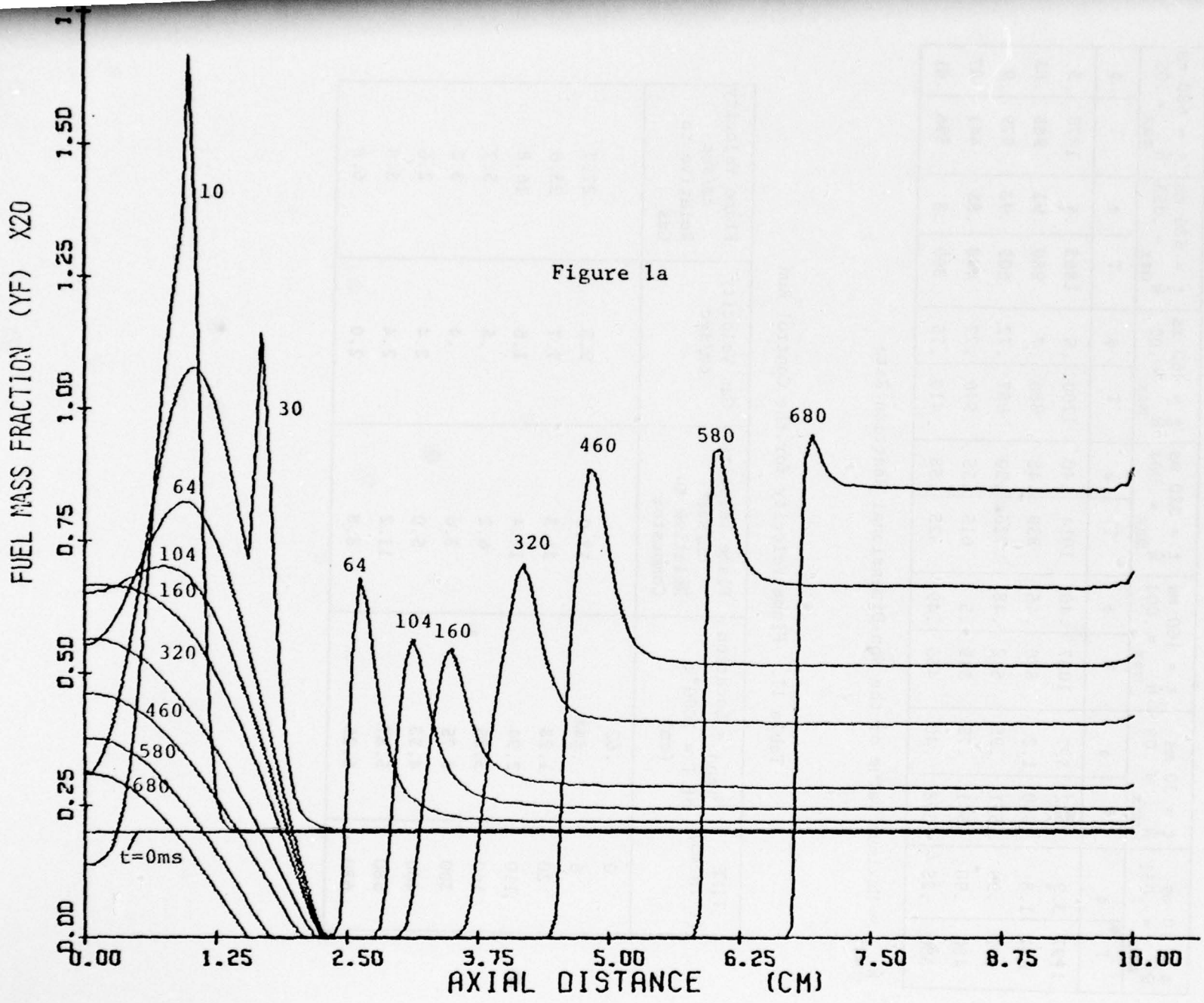

FUEL MASS FRACTION PROFILES

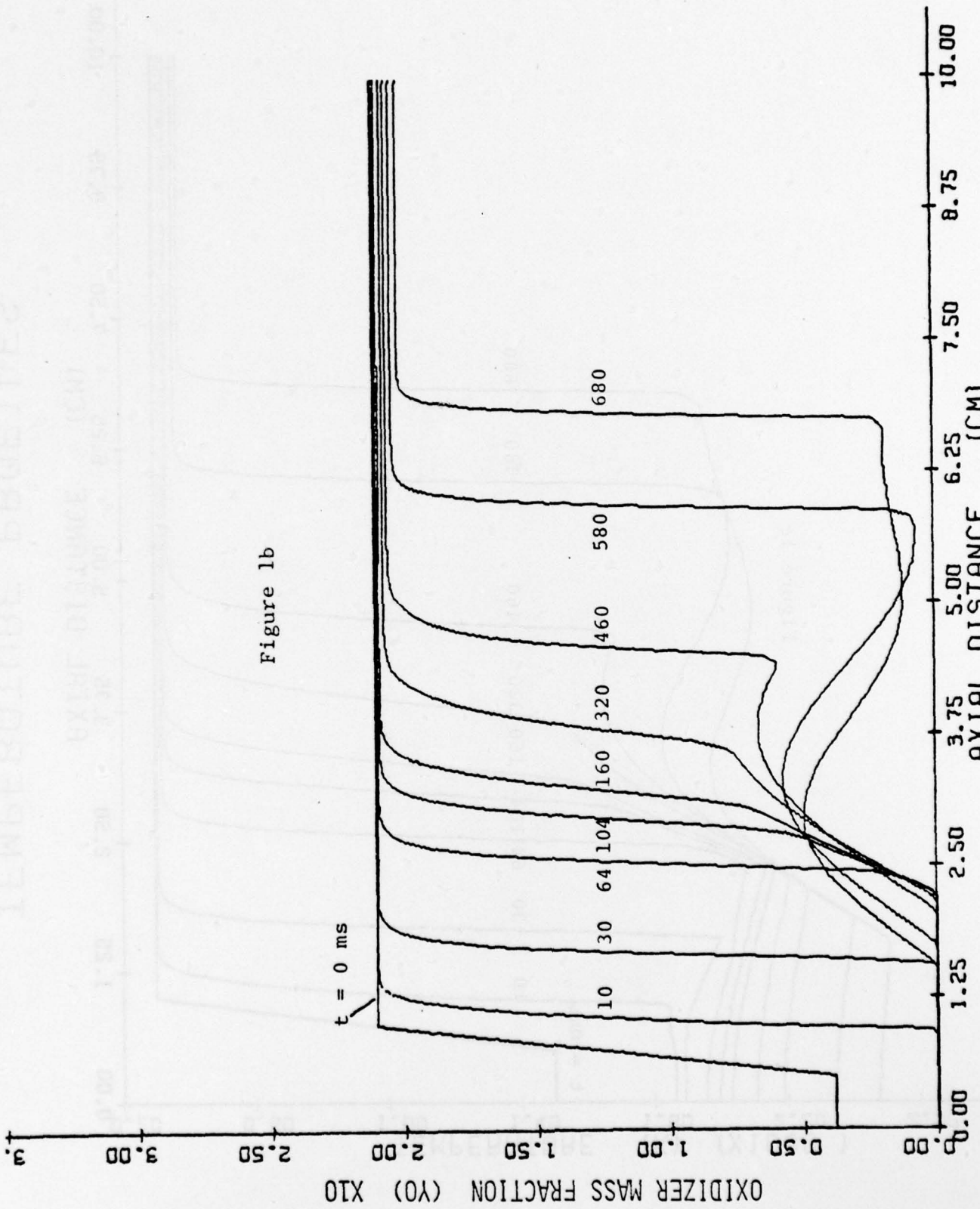
OXIDIZER MASS FRACTION PROFILES
OXIDIZER MASS FRACTION (YO) X10
AXIAL DISTANCE (CM)
t = 0 ms
10
30
64
104
160
320
460
580
680
0.00
1.25
2.50
3.75
5.00
6.25
7.50
8.75
10.00
0.00
0.50
1.00
1.50
2.00
2.50
3.00
3.

Figure 1b

Figure 1c

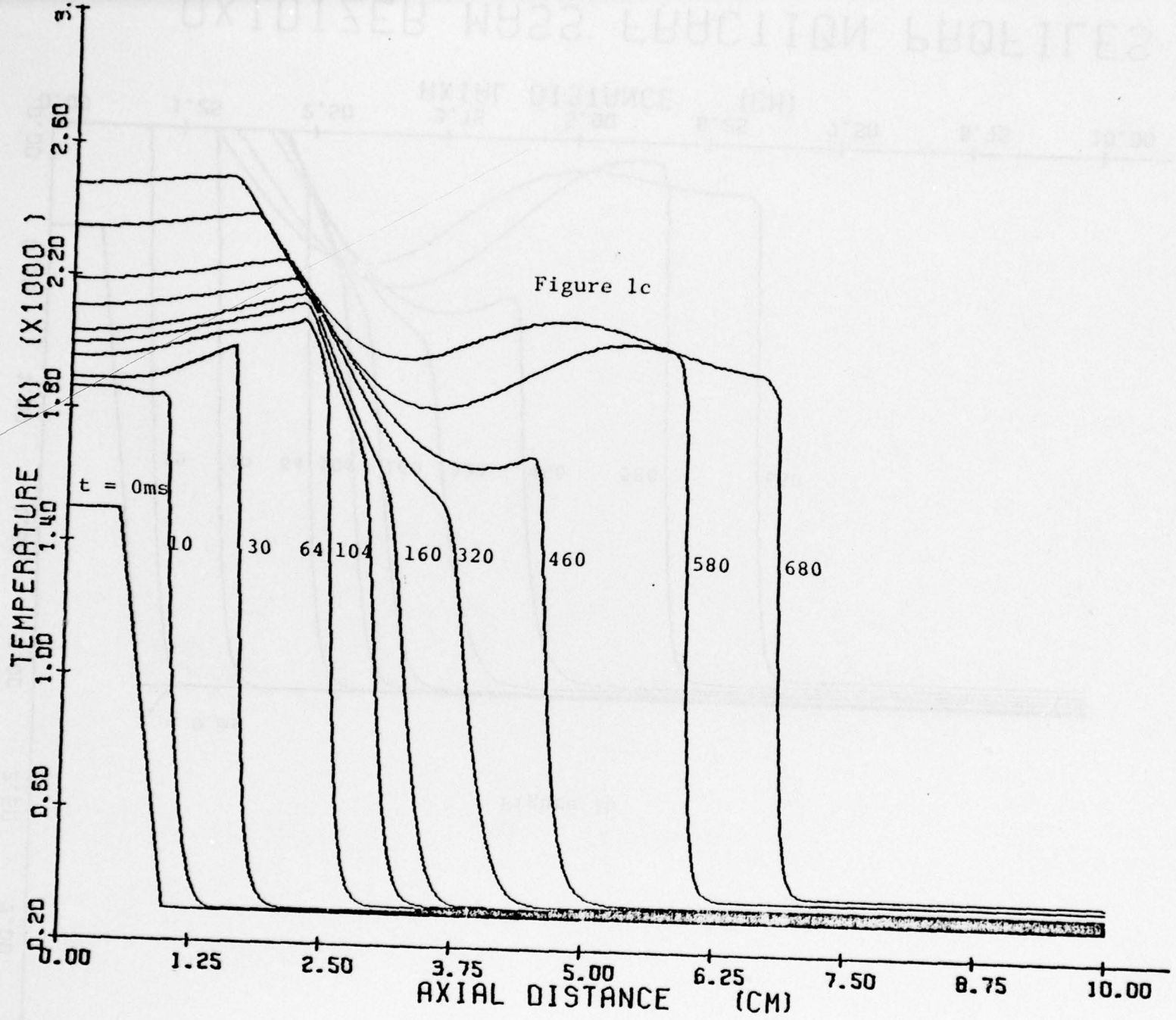

TEMPERATURE PROFILES

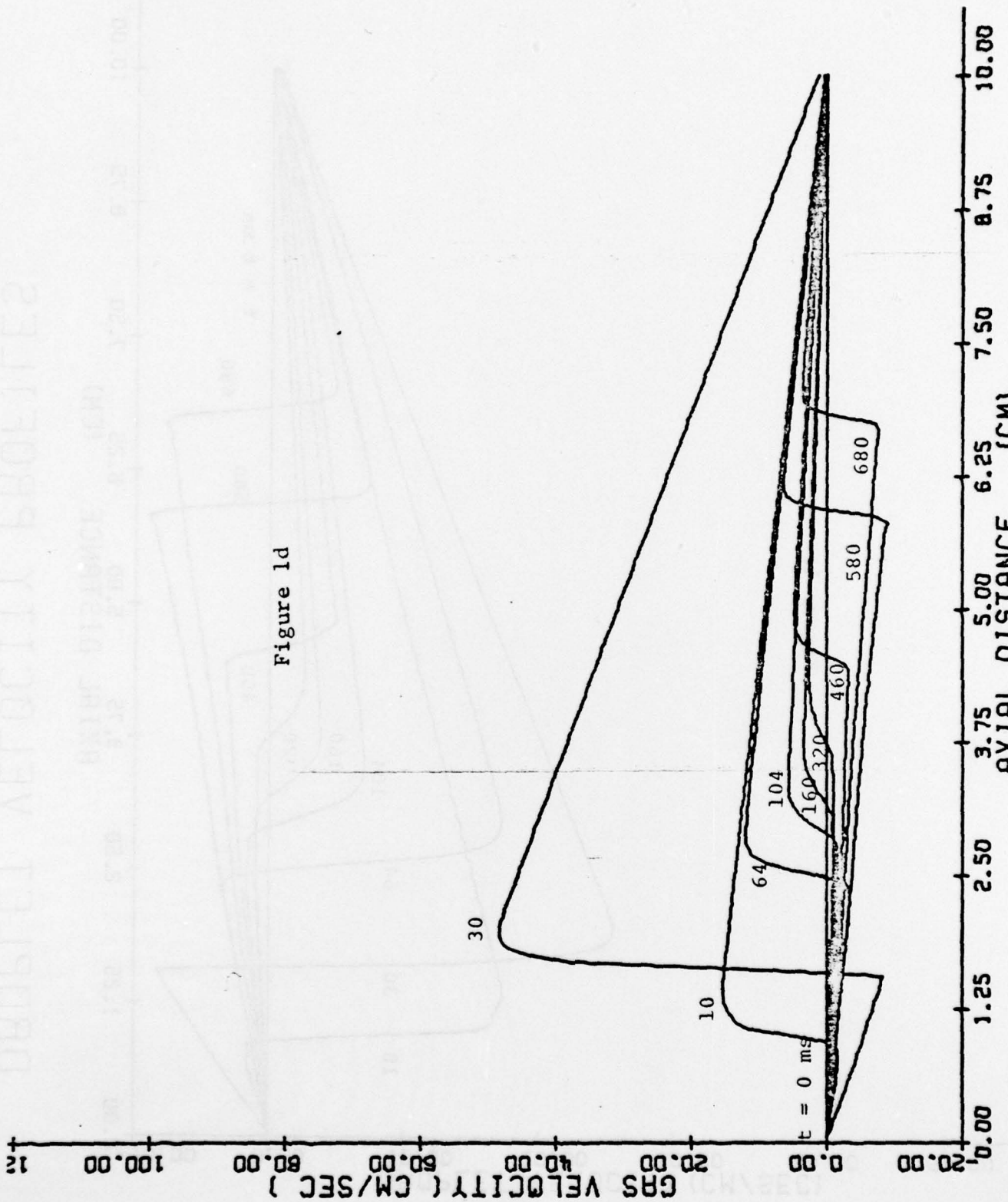
GAS VELOCITY PROFILES
GAS VELOCITY (CM/SEC)
AXIAL DISTANCE (CM)
0.00
1.25
2.50
3.75
5.00
6.25
7.50
8.75
10.00
-20.00
0.00
20.00
40.00
60.00
80.00
100.00
t = 0 ms
10
30
64
104
160
320
460
580
680

Figure 1d

Figure 1e

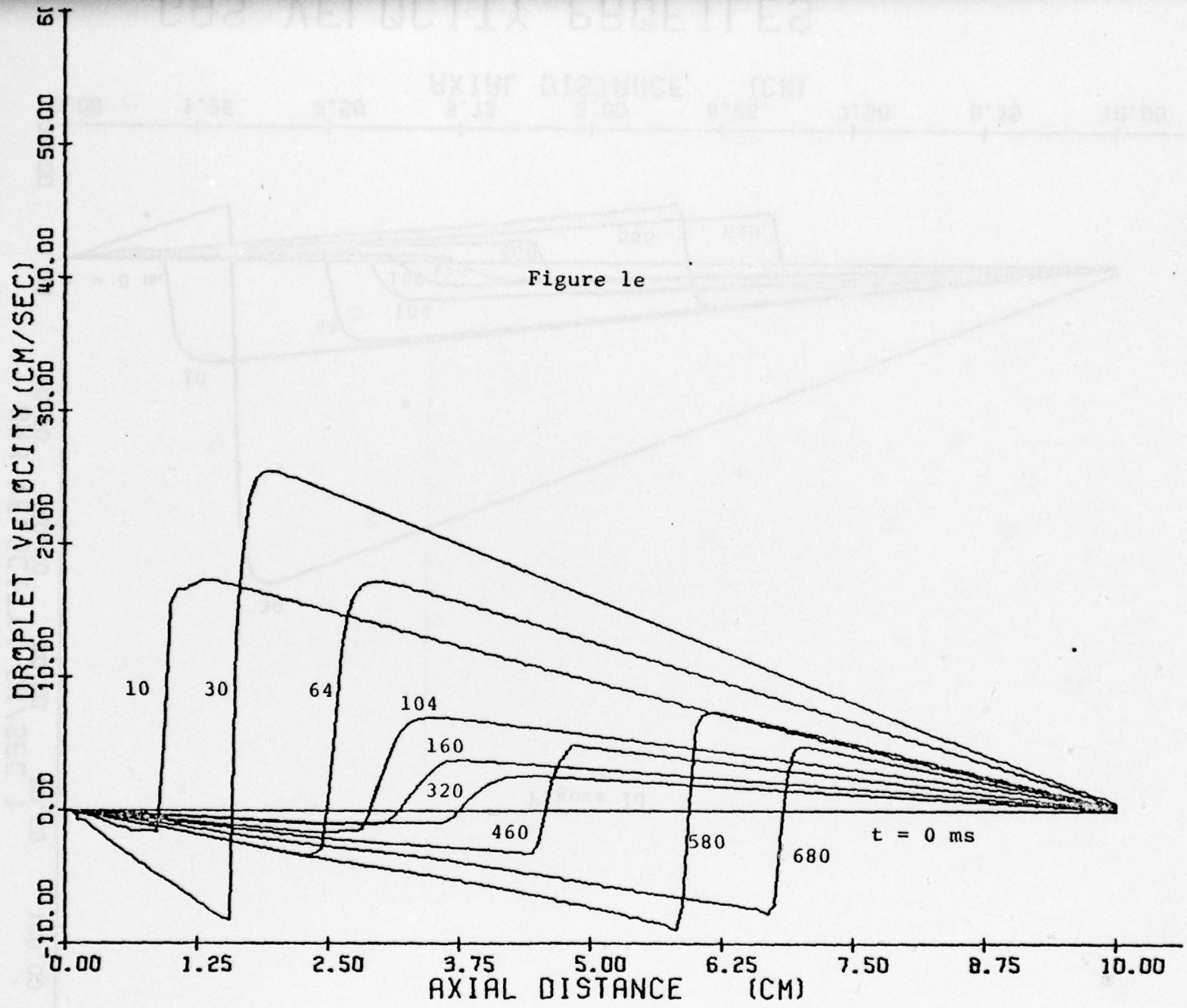

DROPLET VELOCITY PROFILES

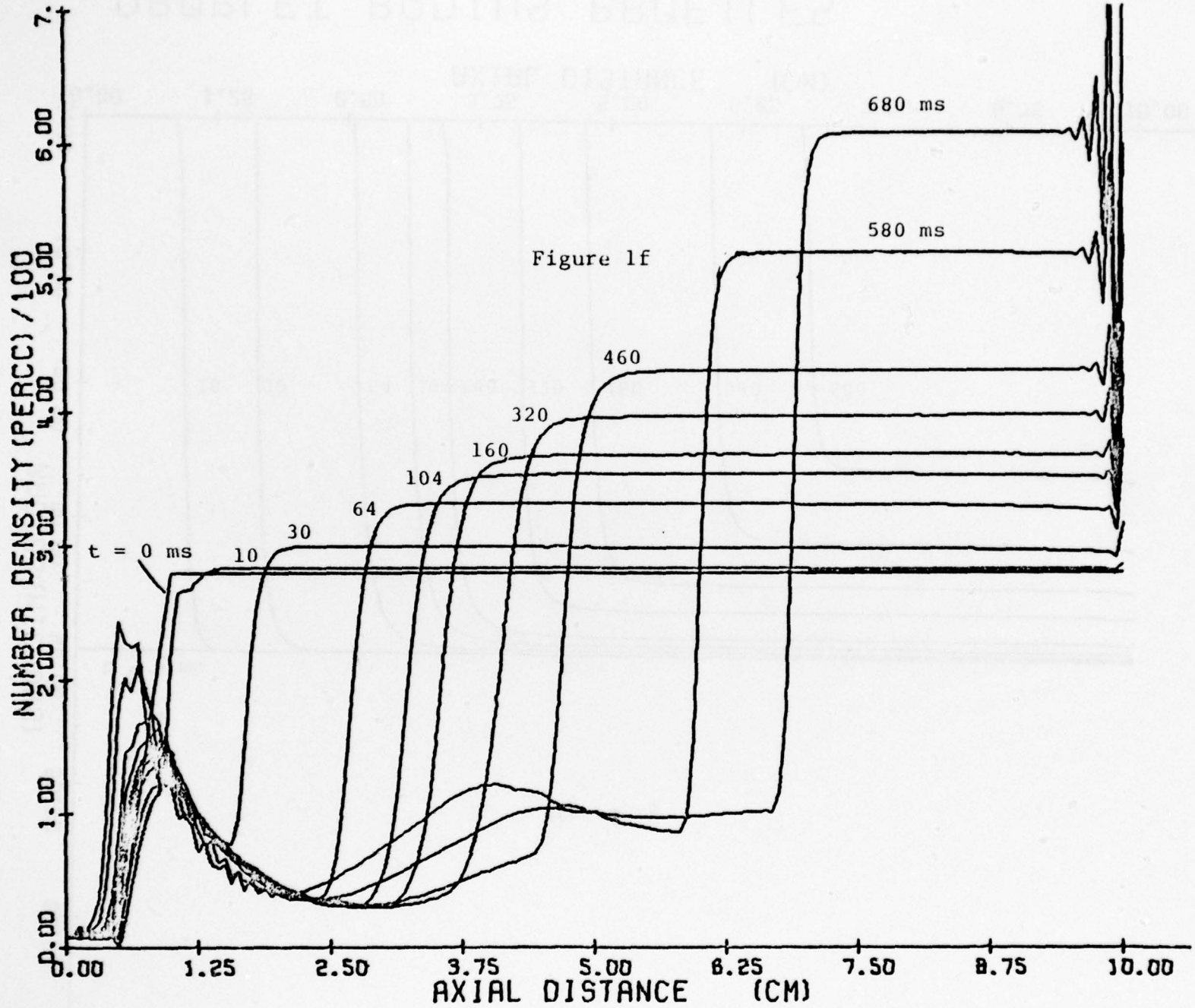

Figure 1f

DROPLET NUMBER DENSITY PROFILES

Figure 1g

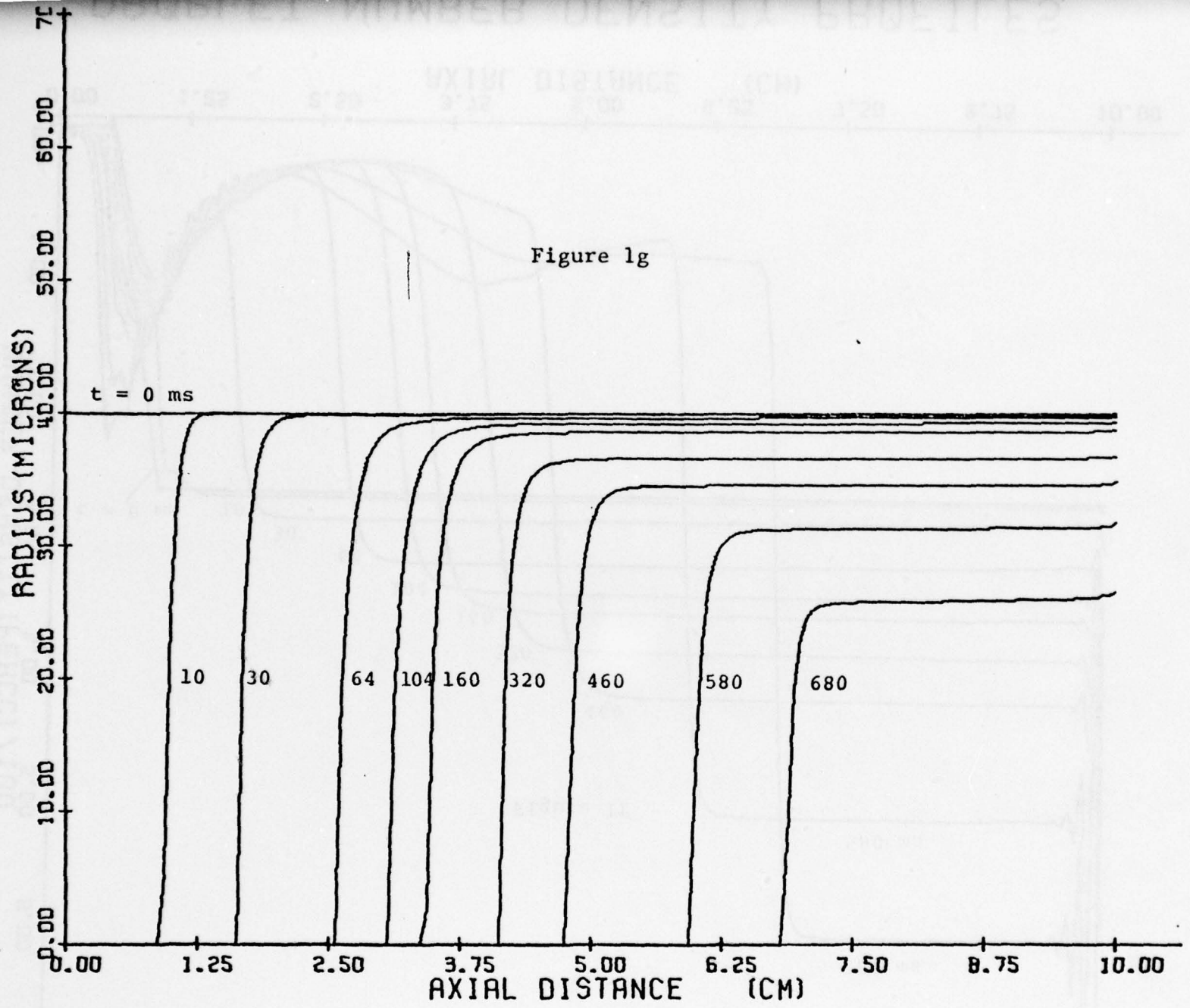

DROPLET RADIUS PROFILES

Figure 1h

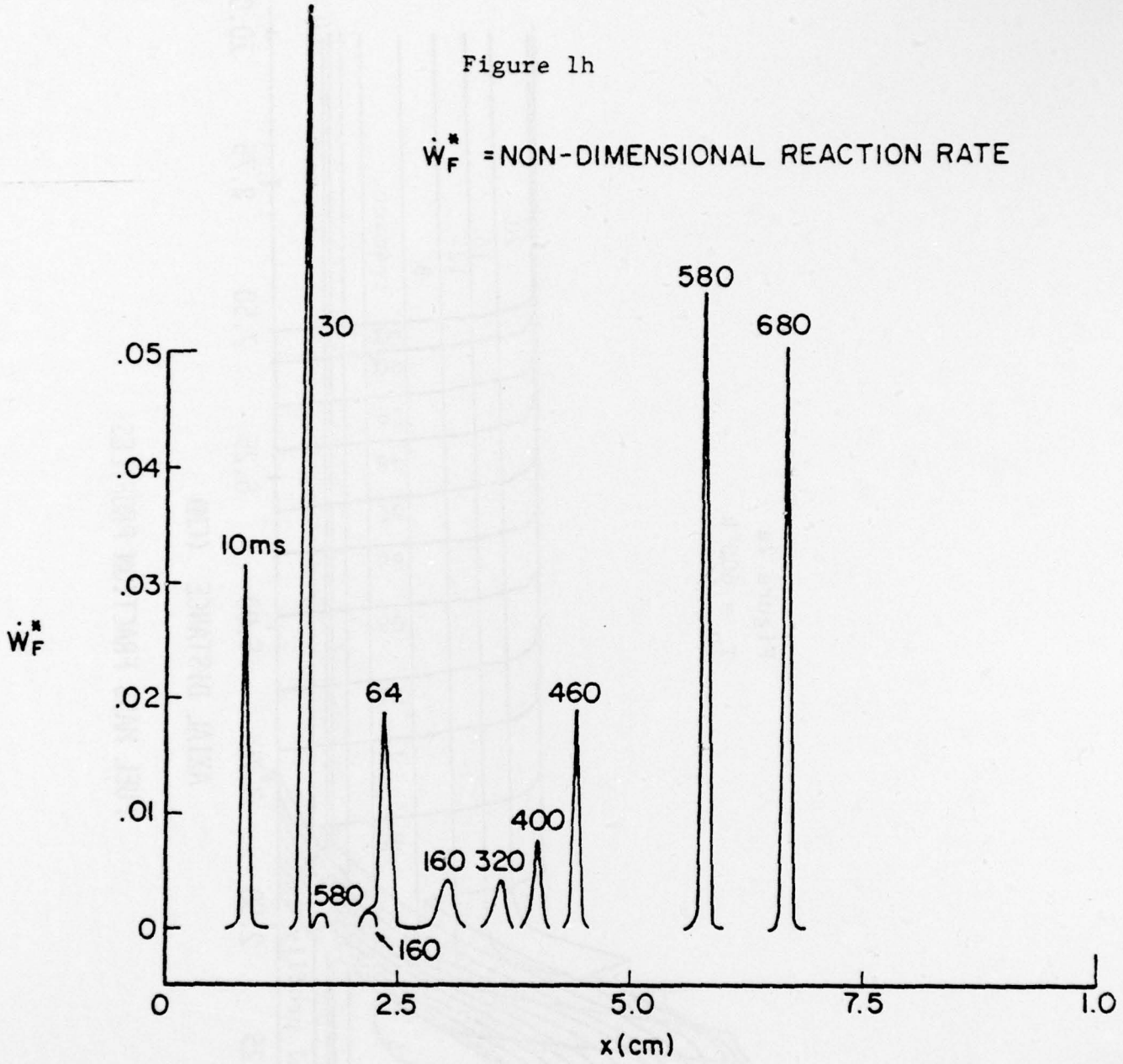

REACTION RATE PROFILES FOR THE CONTROL RUN

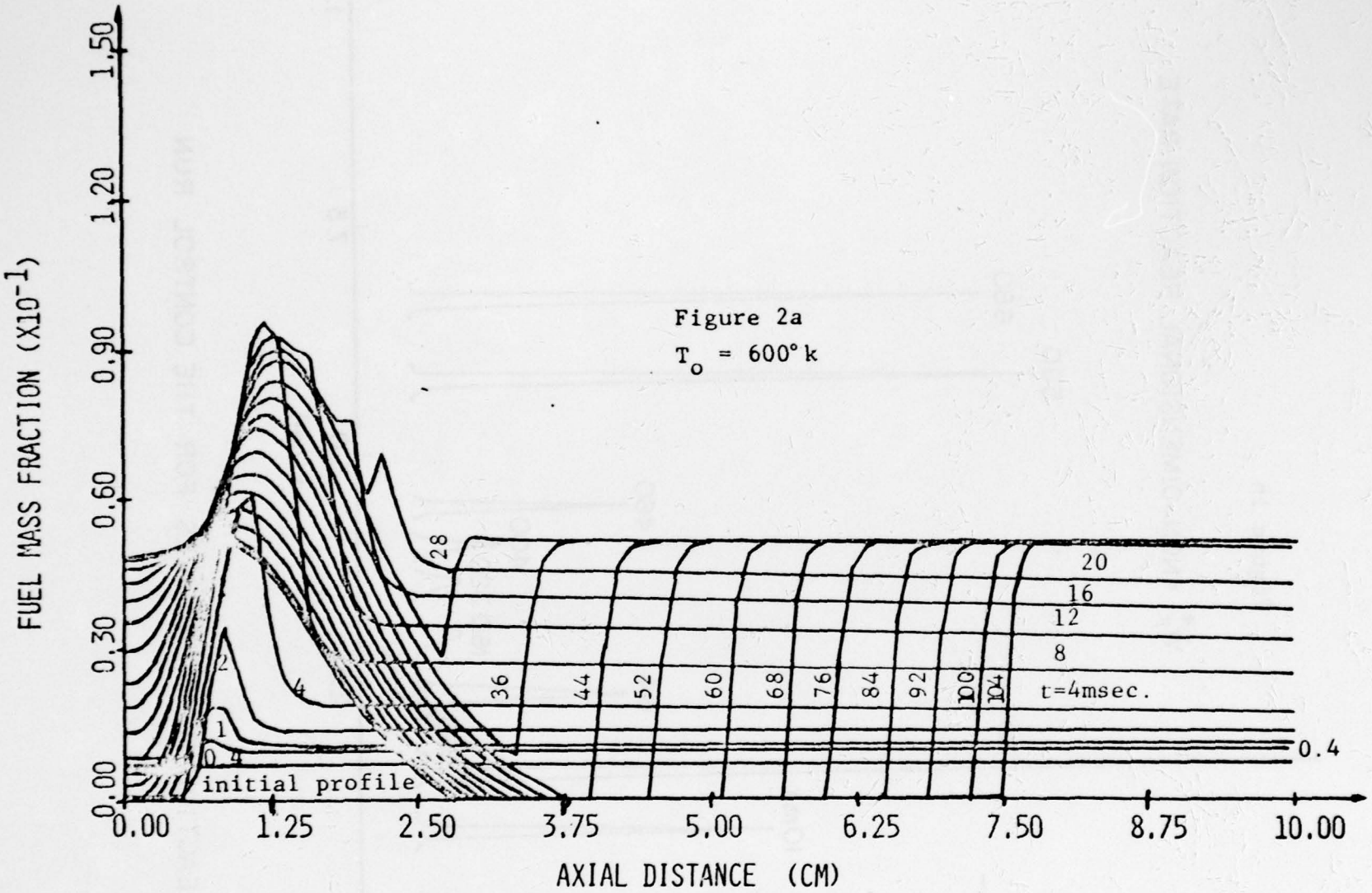

Figure 2a

T_o = 600° k

FUEL MASS FRACTION PROFILES

Figure 2b

T_o = 600°k

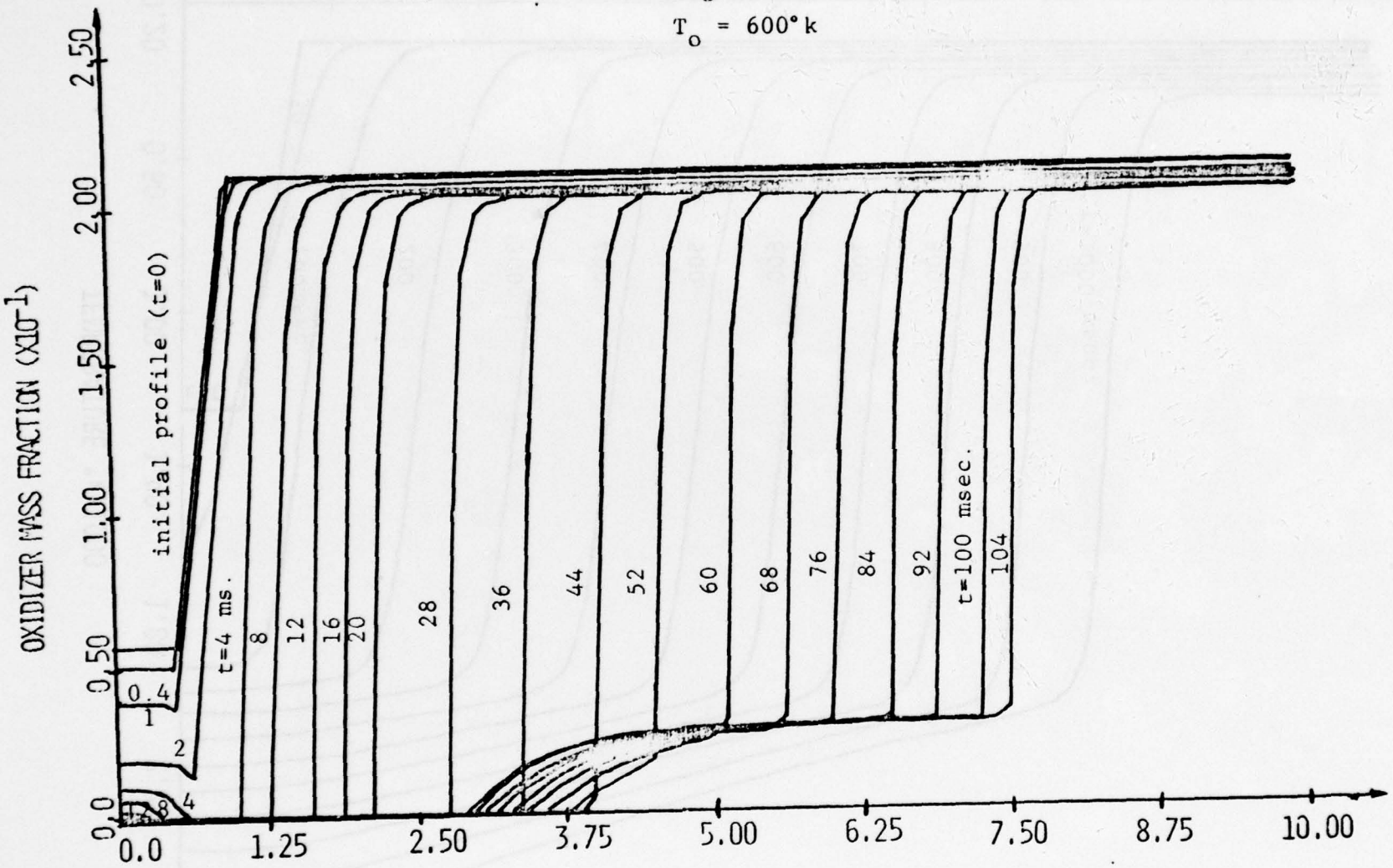

OXIDIZER MASS FRACTION PROFILES

Figure 3

Pre-Mixed Case

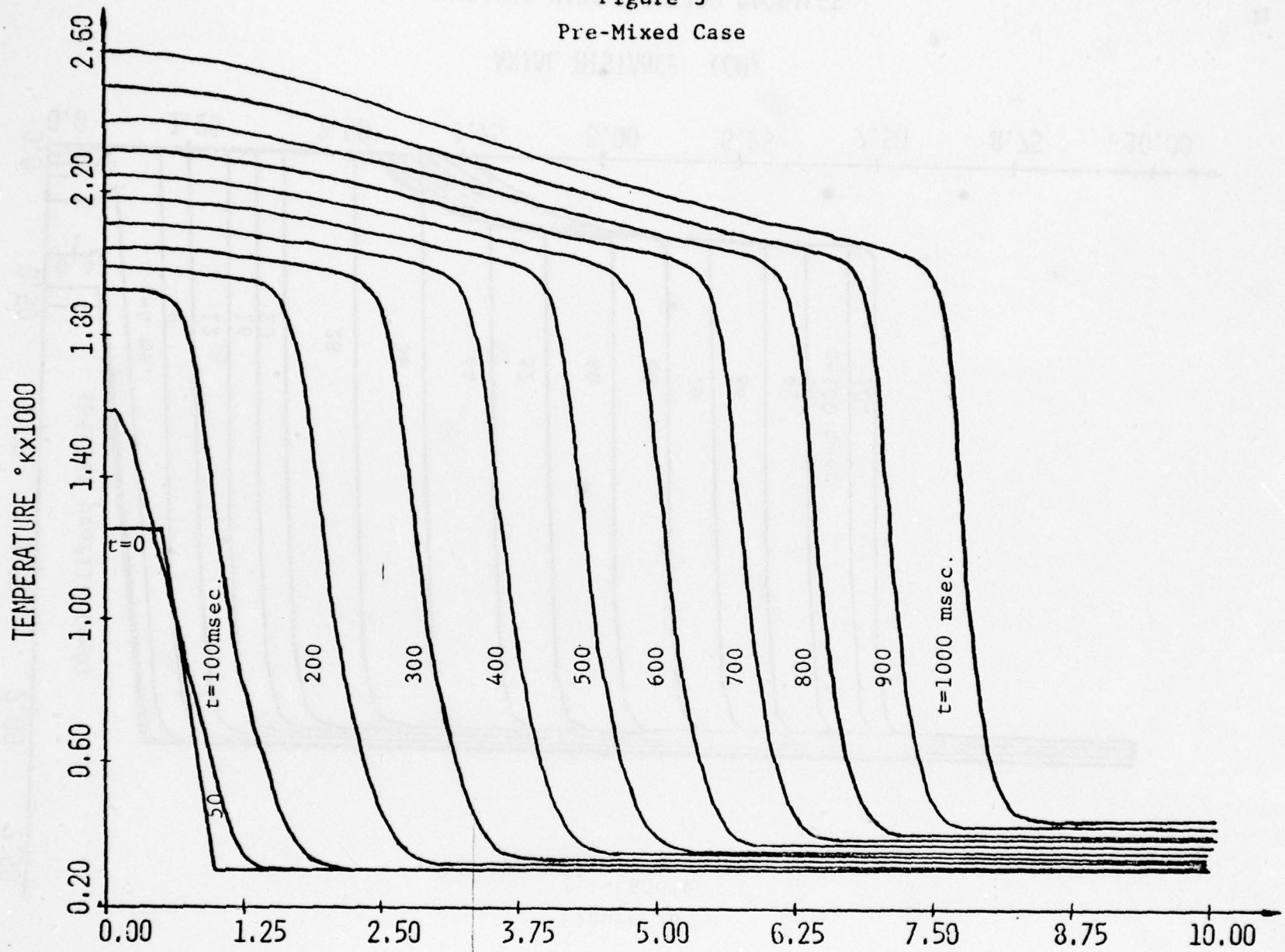

TEMPERATURE PROFILES

Figure 4a

Two Mono-Disperse Droplet Groups

_____Initial Radius 40μ

------Initial Radius 20μ

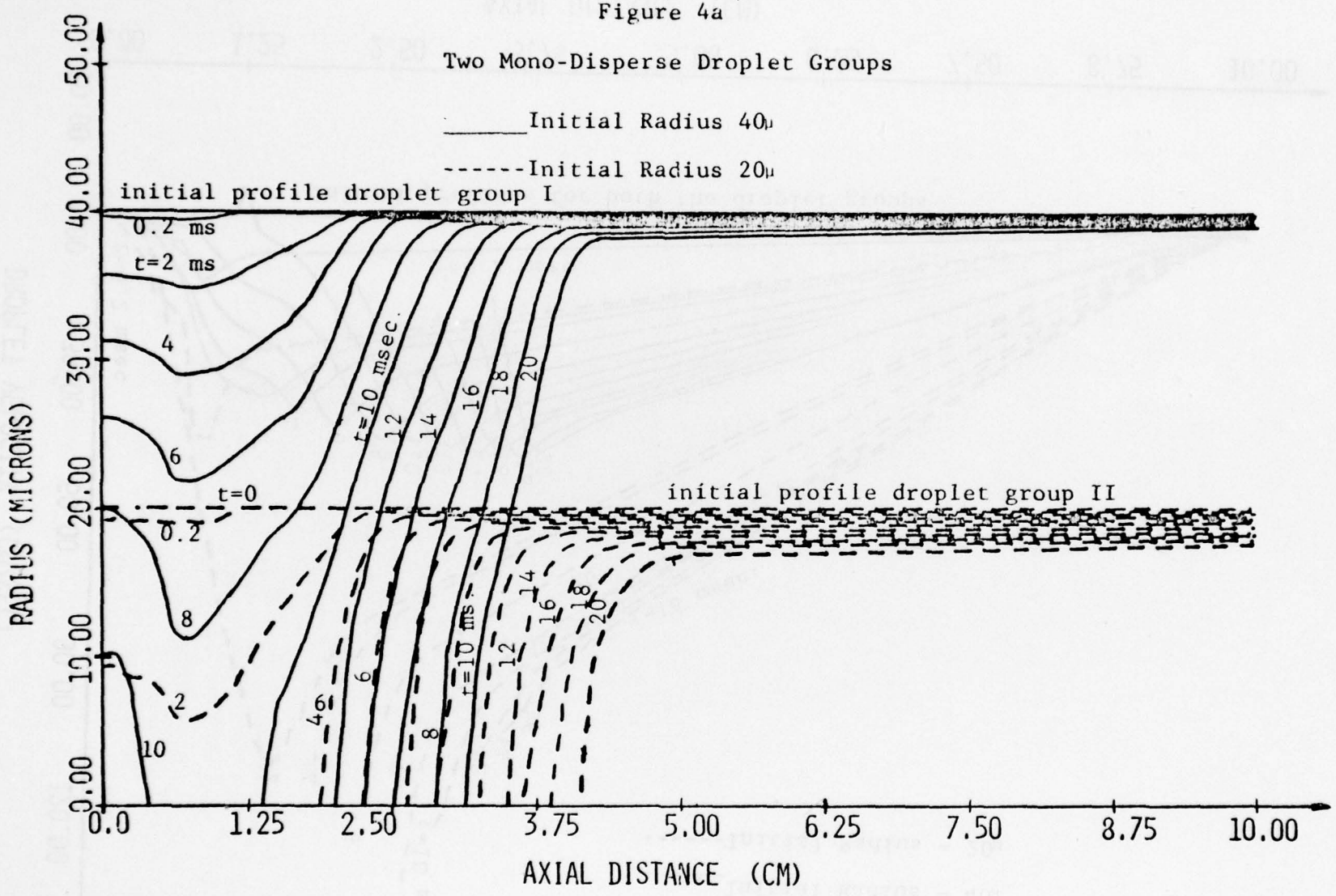

DROPLET RADIUS PROFILES

Figure 4b

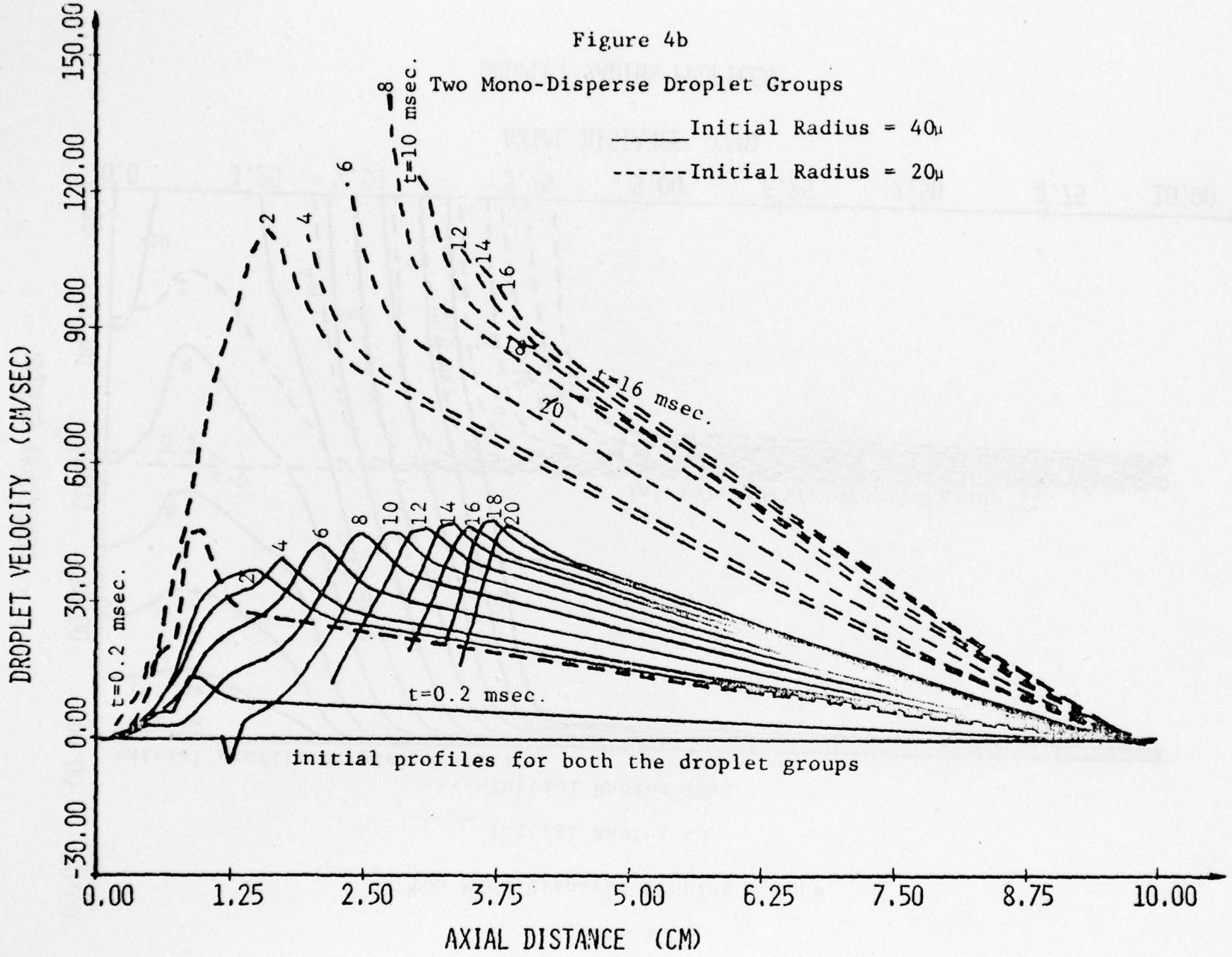

DROPLET VELOCITY PROFILES

1. Wolfhard, H. G. and W. A. Parker, Journal of Industrial Petrol., 35:118 (1949).

2. Burgoyne, J. H. and L. Cohen, Proc. Roy. Soc., A225:357 (1954).

3. Mizutani, Y. and M. Ogasawara, Int. J. Heat & Mass Transfer, 8:921 (1965).

4. Mizutani, Y. and A. Nakajima, Combustion and Flame, 21:343 (1973).

5. Mizutani, Y. and A. Nakajima, Combustion and Flame, 21:351 (1973).

6. Mizutani, Y. and S. Matsushita, Combustion Science and Technology 8:247 (1973).

7. Polymeropoulos, C. E. and S. Das, Combustion and Flame, 25:247 (1975).

8. Hayashi, S. and S. Kumagai, Fifteenth Symposium on Combustion, Williams and Wilkins, Baltimore, 1975.

9. Hayashi, S. and S. Kumagai, Combustion Science and Technology, 15:169 (1977).

10. Williams, F. A., Vol. 2 of Progress in Astronautics and Rocketry, edited by L. E. Bollinger, M. Goldsmith, and A. W. Lemmon, Jr., Academic Press, New York (1960).

11. Mizutani, Y., Combustion Science and Technology, 6:11 (1972).

12. Polymeropoulos, C. E., Combustion Science and Technology, 9:197 (1974).

13. Bracco, F. V., AIChE Symposium Series, 138:70 (1974).

14. Law, C. K., Combustion Science and Technology, 15:65 (1977).

15. Law, C. K., Chemical and Physical Processes in Combustion, The Eastern Section of the Combustion Institute, East Hartford, Nov. 10-11 (1977).

16. Sirignano, W. A., Liquid Propellant Rocket Combustion Instability, D. T. Harrje editor, NASA SP 194 (U.S. Government Printing Office) (October 1972).

17. Law, C. K., Combustion and Flame, 26:17 (1976).

18. Seth, B., M.S.E. Thesis, Princeton University, 1979.

19. Sirignano, W. A., Archives of Thermodynamics and Combustion (1978).

20. Sirignano, W. A. and C. K. Law, Evaporation-Combustion of Fuels, Advances in Chemistry Series 166, ACS (1978).

21. Law, C. K., S. Prakash, and W. A. Sirignano, Proceedings of Sixteenth International Combustion Symposium, Combustion Institute, 1977, p. 605-617.

22. Prakash, S. and W. A. Sirignano, submitted to International Journal of Heat and Mass Transfer (1979).

23. Prakash, S. and W. A. Sirignano, International Journal of Heat and Mass Transfer, 21:7 (1978).

24. Law, C. K. and W. A. Sirignano, Combustion and Flame, 28:175 (1977).

25. Law, C. K., Combustion and Flame, 31:285 (1978).

26. Carslaw, H. S. and J. C. Jaeger, Conduction of Heat in Solids, Oxford University Press, Oxford (1959).

27. Bellman, R. E. and Kalaba, Quasilinearization and Nonlinear Boundary Value Value Problems, American Elsevier Pub. Co., New York, 1965.

28. Lee, E. S., Chemical Engineering Science, 21:143 (1966).

29. Sharma, O. P. and W. A. Sirignano, Combustion Science and Technology, 1:95 (1969).

30. Briley, W. R. and H. McDonald, Journal of Computational Physics, 24:372 (1977).

31. C R C Handbook of Physics and Chemistry 54th Ed., C R C Press.

32. Kanury, M., Introduction to Combustion Phenomena, Gordon & Breach Science Publisher (1975).

33. Reid, Sherwood & Prausnitz, The Properties of Gases and Liquids, McGraw-Hill (1977).